Observed changes in Brewer–Dobson circulation for 1980–2018

To cite this article: Qiang Fu *et al* 2019 *Environ. Res. Lett.* **14** 114026

Environmental Research Letters

LETTER

Observed changes in Brewer–Dobson circulation for 1980–2018

Qiang Fu[1], **Susan Solomon**[2], **Hamid A Pahlavan**[1] **and Pu Lin**[3]

[1] Department of Atmospheric Sciences, University of Washington, Seattle, Washington, United States of America
[2] Department of Earth, Atmospheric, and Planetary Sciences, Massachusetts Institute of Technology, Cambridge, Massachusetts, United States of America
[3] NOAA Geophysical Fluid Dynamics Laboratory/Princeton University, Princeton, New Jersey, United States of America

E-mail: qfu@atmos.washington.edu

Keywords: Brewer–Dobson circulation, ozone depletion and healing, MSU/AMSU

Supplementary material for this article is available online

OPEN ACCESS

RECEIVED
5 July 2019

REVISED
11 October 2019

ACCEPTED FOR PUBLICATION
15 October 2019

PUBLISHED
8 November 2019

Abstract

Previous work has examined the Brewer–Dobson circulation (BDC) changes for 1980–2009 based on satellite Microwave Sounding Unit (MSU/AMSU) lower-stratospheric temperature (T_{LS}) observations and ERA-Interim reanalysis data. Here we examine the BDC changes for the longer period now available (1980–2018), which also allows analysis of both the ozone depletion (1980–1999) and ozone healing (2000–2018) periods. We provide observational evidence that the annual mean BDC accelerated for 1980–1999 but decelerated for 2000–2018, with the changes largely driven by the Southern Hemisphere (SH), which might be partly contributed by the effects of ozone depletion and healing. We also show that the annual mean BDC has accelerated in the last 40 years (at the 90% confidence level) with a relative strengthening of ~1.7% per decade. This overall acceleration was driven by both Northern Hemisphere (40%) and SH (60%) cells. Significant SH radiative warming is also identified in September for 2000–2018 after excluding the year 2002 when a very rare SH stratospheric sudden warming occurred, supporting the view that healing of the Antarctic ozone layer has now begun to occur during the month of September.

1. Introduction

The global residual circulation of the stratosphere—the Brewer–Dobson circulation (BDC)—consists of a meridional cell in each hemisphere, with air rising across the tropical tropopause, moving poleward, and sinking into the extratropical troposphere (e.g. Holton *et al* 1995, Plumb 2002, Butchart 2014). Brewer (1949) and Dobson (1956) first proposed this circulation to explain the observed stratospheric water vapor and ozone distributions. By moving air into and out of the stratosphere, the BDC sets the mean age or the residence time of air in the stratosphere (e.g. Hall and Plumb 1994). The BDC affects the distribution and abundance of stratospheric ozone directly by transporting ozone from the tropics to polar regions, and indirectly through its effect on ozone chemistry via temperature changes and transport of other chemical species (e.g. Dobson 1956, Shepherd 2008). The BDC determines the stratosphere-to-troposphere ozone flux on the global and hemispheric scales (e.g. Holton 1990, Holton *et al* 1995, Appenzeller *et al* 1996). The BDC directly modulates the tropical tropopause temperatures, tropical tropopause layer cirrus, and stratospheric water vapor, all of which are associated with climate change processes (Birner 2010, Davis *et al* 2013, Dessler *et al* 2013, Fu 2013, Tseng and Fu 2017).

In the last 15 years, there has been a surge of interest in the BDC mainly resulting from the development and continuing improvements of general circulation models (GCMs) and chemistry-climate models (CCMs) with detailed representations of the stratosphere (e.g. Pawson *et al* 2000, Eyring *et al* 2005, Gerber *et al* 2012, Butchart 2014). In agreement with the pioneering work by Rind *et al* (1990), the stratosphere-resolving GCMs and CCMs consistently predict a strengthening of the BDC in response to greenhouse gas (GHG)-induced climate change (e.g. Butchart *et al* 2006, Garcia and Randel 2008, Li *et al* 2008, McLandress and Shepherd 2009, Okamoto *et al* 2011, Bunzel and Schmidt 2013, Lin and Fu 2013,

Oberlander *et al* 2013), making it one of the robust manifestations of projected GHG-induced climate change. Several modeling studies also find that the BDC becomes stronger (weaker) in response to the ozone depletion (recovery) (e.g. Shindell and Schmidt 2004, Li *et al* 2008, Oman *et al* 2009, McLandress *et al* 2010, Polvani *et al* 2011, Lin and Fu 2013, Polvani *et al* 2018, Polvani *et al* 2019).

It is essential that such model predictions be checked against all relevant observations. The BDC strength and its changes cannot be measured directly, but can be inferred from observations. Changes in the BDC strength have been examined on the decadal time scale from observations of age of stratospheric air (e.g. Engel *et al* 2009, Stiller *et al* 2012, Haenel *et al* 2015, Engel *et al* 2017, Stiller *et al* 2017), but it has become clear now that changes in mean age of stratospheric air do not constrain residual circulation changes since they represent a combination of changes in mixing and in residual transport (Garny *et al* 2014, Ray *et al* 2014, Ploeger *et al* 2015, Dietmüller *et al* 2017). On the other hand, an accelerated (decelerated) BDC leads to a cooling (warming) of the tropical lower stratosphere and warming (cooling) in high latitudes, due to the close relationship between variations of temperatures and residual vertical velocities in the lower stratosphere (e.g. Yulaeva *et al* 1994). Observational evidence of a long-term BDC strengthening has been suggested over both the tropics and high latitudes based on consistent changes in lower stratospheric temperatures (Thompson and Solomon 2005, Johanson and Fu 2007, Hu and Fu 2009, Lin *et al* 2009, Thompson and Solomon 2009, Fu *et al* 2010, Young *et al* 2012, Fu *et al* 2015, Osso *et al* 2015). Further, Fu *et al* (2015) examined the BDC changes for 1980–2009 using satellite Microwave Sounding Unit (MSU/AMSU) lower-stratospheric temperature (T_{LS}) observations along with ERA-Interim reanalysis data. They found that the annual mean BDC accelerated (at 90% confidence) with a relative strengthening of ~2.1% per decade and with most of the change coming from the Southern Hemisphere (SH). Here we provide important new information on BDC changes using the full record for 1980–2018 as well as partitioning it into 1980–1999 (ozone depletion) and 2000–2018 (ozone healing) periods. We find that the annual mean BDC accelerated for 1980–1999 but decelerated for 2000–2018, with almost all the changes coming from the SH. We also show that the annual mean BDC accelerated in the last 40 years (at 90% confidence) with a relative strengthening of ~1.7% per decade, contributed by both Northern Hemisphere (NH) (40%) and SH (60%) cells. Significant SH radiative warming in September for 2000–2018 after excluding the year 2002 is also shown, further supporting a key role for the healing of the Antarctic ozone layer that has now begun to occur particularly during the month of September (see Solomon *et al* 2016).

2. Data and methods

The data and methods used in this study closely follow Fu *et al* (2015), which are only briefly described here. We used the most recent version of the satellite MSU/AMSU lower stratospheric temperature (T_{LS}) dataset (v4.1) compiled by the National Oceanic and Atmospheric Administration team (Zou *et al* 2018). It is gridded at 2.5° latitude by 2.5° longitude, extending from 82.5°N to 82.5°S. We define the tropics as the region from 20°S to 20°N and high latitudes as latitudes from 40°N(S) to 82.5°N(S) (Fu *et al* 2010, Fu *et al* 2015). Similar results were obtained by employing the T_{LS} datasets from the Remote Sensing System team (Mears and Wentz 2017) and the University of Alabama at Huntsville team (Spencer *et al* 2017) (not shown). The results in Fu *et al* (2015) were reproduced (not shown), indicating little sensitivity to the T_{LS} dataset version used.

The 6 hourly ERA-Interim reanalysis data (Dee *et al* 2011) were used to calculate the eddy heat flux as an index of the strength of the BDC (Lin *et al* 2009, Fu *et al* 2010, Fu *et al* 2015). It is averaged over 3 months, including the given month and two previous months and over the high latitudes of each hemisphere (40°S–90°S and 40 °N–90°N), and is vertically averaged between 10 and 50 hPa. Fu *et al* (2015) considered the period of 30 years from 1980 to 2009, with the starting year to avoid the need of reanalysis data prior to the satellite era. Here we consider the period of 39 years from 1980 to 2018. In addition, we consider 20 and 19 years of the ozone depletion (1980–1999) and healing (2000–2018) periods (Solomon *et al* 2016, Solomon *et al* 2017), respectively.

The observed high-latitude T_{LS} trends were separated into a dynamical component due to the change of the BDC and a radiative component due to the change of radiatively active trace species (Fu *et al* 2010, Fu *et al* 2015) as well as solar activity. A regression of gridded T_{LS} data was performed upon the corresponding eddy heat flux index time series for each month and over each hemisphere. The attribution of the T_{LS} trends to changes in the BDC was derived by multiplying the regression maps with the linear trends obtained in the eddy heat flux index as in Fu *et al* (2015). The T_{LS} trends due to the BDC changes were averaged over high latitudes in each hemisphere for each month. The radiative component, averaged over 40–82.5°S(N), was derived as the observed total T_{LS} trend minus the dynamical component, averaged over the same regions. The confidence intervals in the derived trends were determined using a Monte Carlo method (Fu *et al* 2015). The method for separation of observed T_{LS} trends over the tropics into the radiative and BDC change-induced dynamical components will be described when the results are given in the next section. The radiative component of tropical T_{LS} trends derived from the MSU/AMSU observations along with the ERA-Interim reanalysis is

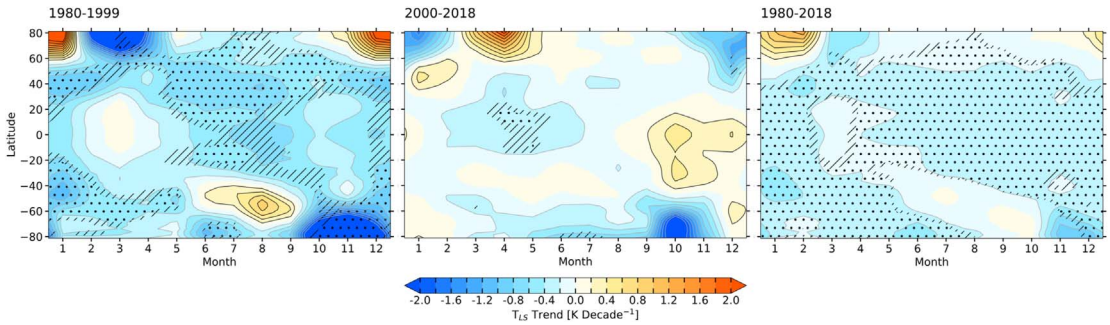

Figure 1. Zonal mean lower-stratospheric temperature (T_{LS}) trends for 1980–1999 (left), 2000–2018 (middle), and 1980–2018 (right) versus month and latitude from MSU/AMSU observations. The area where the trend is significant at 95% (90%) confidence levels is indicated by dots (slant lines).

independently validated both in terms of its small seasonal dependence and annual mean value (Fu *et al* 2015). See Lin *et al* (2009), Fu *et al* (2010) and Fu *et al* (2015) for more details on the justification of using the reanalysis eddy heat flux trends.

3. Results

Figure 1 shows the zonal mean T_{LS} trend versus month and latitude for 1980–1999 (left), 2000–2018 (middle), and 1980–2018 (right), which are driven by a combination of the direct radiative effects due to atmospheric composition changes and solar activity, and the BDC-induced temperature changes (Fu *et al* 2015). Radiative cooling trends prevail for 1980–1999 because of ozone depletion, GHG increases, stratospheric aerosols from the El Chichon volcanic eruption in March 1982 and Pinatubo in June 1991, and solar activity (see time series of stratospheric aerosols and solar activities in figure SM1 is available online at stacks.iop.org/ERL/14/114026/mmedia). There is a particularly strong cooling trend poleward of 60°S during October—December, which was caused by the Antarctic ozone hole (Solomon 1999). A slightly positive trend over the tropics in March indicates a strong dynamical warming that cancels direct radiative cooling there, and is related to strong dynamical cooling in the NH high latitudes in the same month. The dynamical cooling in March in the NH high latitudes could be related to a delay in the final warming (i.e. the polar vortex breakdown). The T_{LS} warming in the SH high-latitude winter/spring seasons and in the NH high-latitude winter is coupled to enhanced cooling in the tropics and is also consistent with BDC changes. Similar T_{LS} trend patterns were observed for 1980–2018 (right panel in figure 1) but with smaller magnitudes (also see figure 2 in Fu *et al* 2010 for 1980–2008). The behavior for 2000–2018 is strikingly different from the first period. It is known that there is much less volcanic aerosol effect then, and a radiative warming is expected due to the ozone healing (Solomon *et al* 2016, Solomon *et al* 2017). Furthermore, a stepwise drop of tropical lower-stratospheric water vapor concentration in 2000, which persisted until late 2005 and then started to increase gradually back (Randel *et al* 2006, Fueglistaler 2012, Ding and Fu 2018), would lead to a radiative cooling trend. Overall the radiative trends for 2000–2018 are much smaller than 1980–1999. While the comparison of the trend patterns between 2000–2018 and 1980–1999 suggests that the BDC changes might have opposite signs for these two periods, a quantitative estimate of the BDC change requires the separation of the dynamical and radiative components in T_{LS} trends, which will be discussed next.

Figure 2 shows the zonal-mean annual-mean T_{LS} trend versus latitude for 1980–1999 (blue), 2000–2018 (red), and 1980–2018 (black). The enhanced cooling in the midlatitudes during 1980–1999 was associated with tropical expansion (Fu *et al* 2006, Fu and Lin 2011). A full interpretation of figure 2 also requires the separation of dynamical and radiative components (Lin *et al* 2009, Fu *et al* 2010, Bohlinger *et al* 2014, Fu *et al* 2015, Ivy *et al* 2016, Maycock *et al* 2018).

The blue lines in figure 3 show the T_{LS} trends due to BDC changes (see Data and Methods section), averaged over high latitudes of 40–82.5 °S and 40–82.5 °N, versus month, while the red lines show observed T_{LS} trends over the tropics. A strong anti-correlation between observed tropical T_{LS} trends and high-latitude T_{LS} dynamical components indicates that the monthly dependence of observed tropical T_{LS} trend is indeed largely driven by the BDC changes for all three periods considered. Following Fu *et al* (2015), the observed T_{LS} trends in the tropics are next separated into two parts as T_{LS}(Tropics) = aT_{LS}(High-Lat, Dyn) + [T_{LS}(Tropics) − aT_{LS}(High-Lat, Dyn)]. Here a is a coefficient obtained from orthogonal least squares fitting between the observed tropical T_{LS} trends, i.e. T_{LS}(Tropics), and high-latitude T_{LS} dynamical components, i.e. T_{LS}(High-Lat, Dyn). The observed T_{LS} trends in the tropics are thus separated into the BDC change-induced dynamical components and empirically derived radiative components (i.e. black lines in figure 3), corresponding to the first and

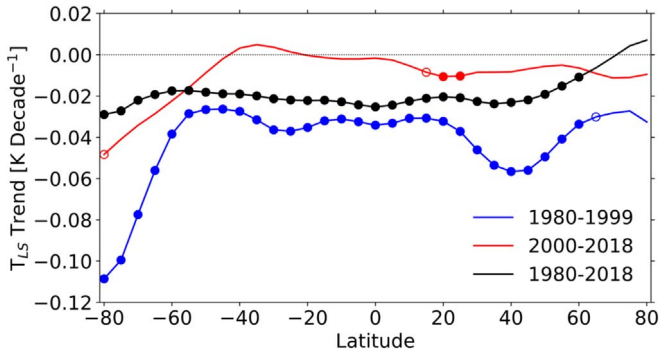

Figure 2. Lower-stratospheric temperature (T_{LS}) trend as a function of latitude based on zonal-mean T_{LS} temperature anomaly time series for 1980–1999 (blue), 2000–2018 (red), and 1980–2018 (black) from MSU/AMSU observations. The trends are shown as filled (open) circles when they are significant at the 95% (90%) confidence levels.

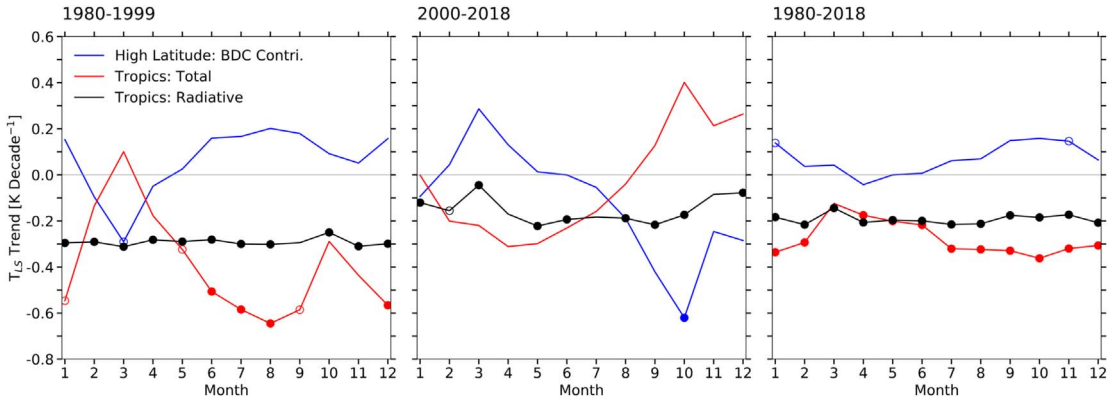

Figure 3. The lower-stratospheric temperature (T_{LS}) trends due to changes of the Brewer–Dobson circulation (BDC) over combined high latitudes (40°N–82.5°N and 40°S–82.5°S) (blue lines) and MSU/AMSU-observed T_{LS} trends in the tropics (20°N–20°S) (red lines) along with its estimated radiative component (black lines), versus month, for 1980–1999 (left), 2000–2018 (middle), and 1980–2018 (right). The trends are shown as filled (open) circles when they are significant at the 95% (90%) confidence levels.

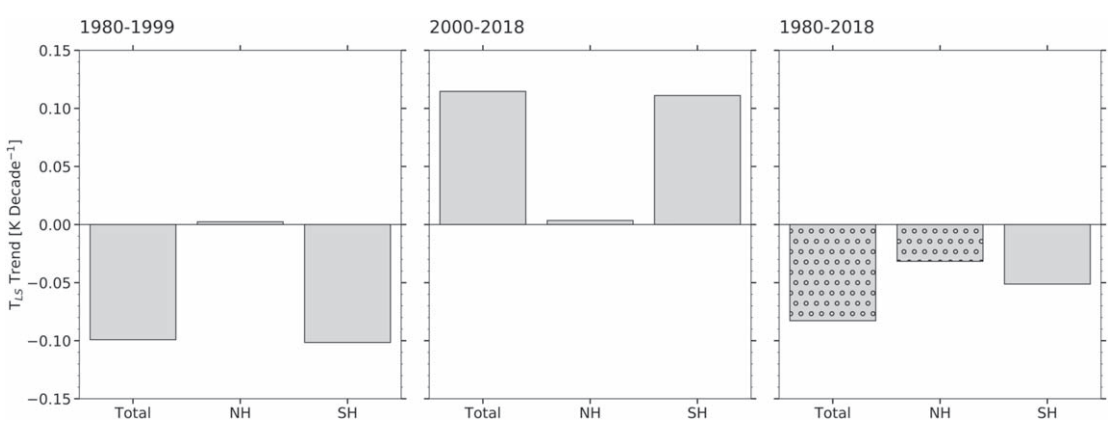

Figure 4. Annual mean lower-stratospheric temperature (T_{LS}) trend in the tropics (20°N–20°S) due to changes of the BDC and the contribution from the Northern Hemisphere (NH) and Southern Hemisphere (SH) cells for 1980–1999 (left), 2000–2018 (middle), and 1980–2018 (right). The trend bars marked with open circles are significant at the 90% confidence levels.

second terms on the right-hand side of the above equation, respectively. Figure 3 shows a weakening of the BDC in boreal spring and a strengthening in other seasons for 1980–1999 but opposite behavior for 2000–2018. For 1980–2018, the BDC is strengthened in July–January but shows little change in February–June. The derived annual mean radiative components of tropical T_{LS} are −0.29, −0.15, and −0.19 K/decade, respectively, for 1980–1999, 2000–2018, and 1980–2018.

The BDC change-induced T_{LS} annual mean trend and the contributions from the NH and SH cells are

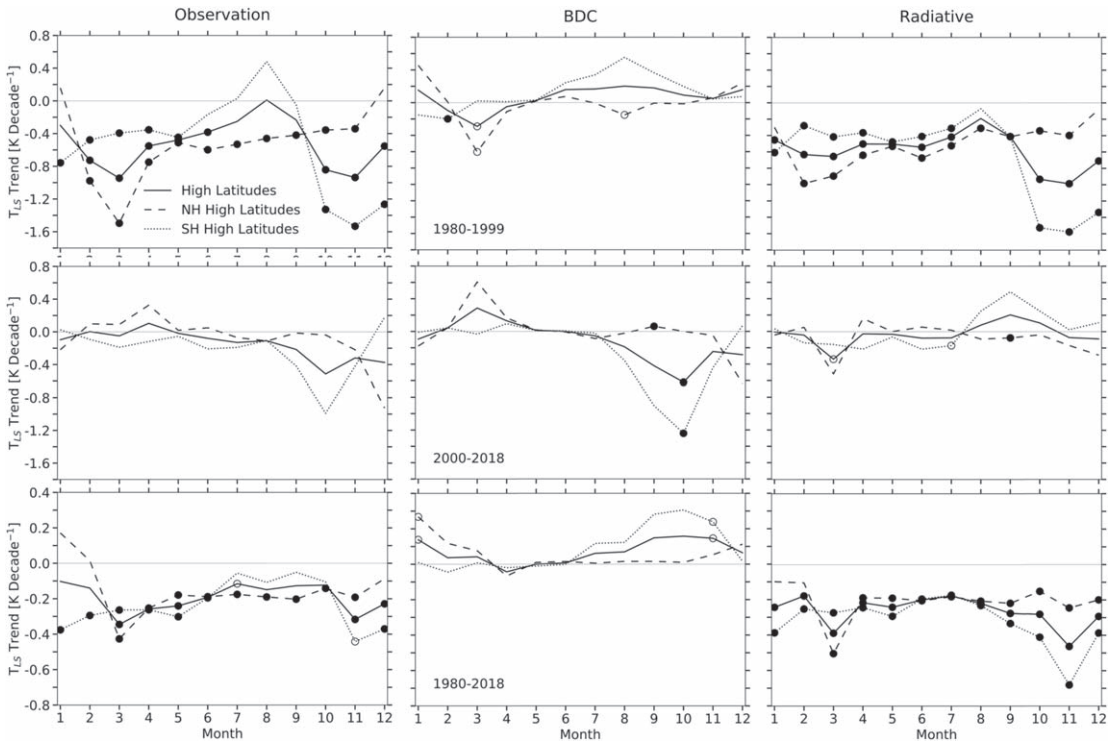

Figure 5. Lower stratospheric temperature (T_{LS}) trends versus month for MSU/AMSU-observed total (left), BDC-induced dynamical contributions (middle), and radiative contributions (right) over 1980–1999 (upper), 2000–2018 (middle), and 1980–2018 (lower) for SH high latitudes (40°S–82.5°S, dotted lines), NH high latitudes (40°N–82.5°N, dashed lines), and combined high latitudes (40°N–82.5°N and 40°S–82.5°S, solid lines). The trends are shown as filled (open) circles when they are significant at the 95% (90%) confidence levels.

shown in figure 4 over the tropics. The tropical NH and SH contributions to the BDC trends were computed by multiplying the corresponding high-latitude NH and SH dynamical contributions by the coefficient *a*. The BDC change-induced T_{LS} annual mean trends in the tropics are −0.10, 0.11, and −0.08 K/decades for 1980–1999, 2000–2018, and 1980–2018, respectively, indicating a strengthening, weakening, and strengthening of the BDC. The BDC changes in the first and second periods are almost entirely caused by the SH cells (figure 4). For the overall period 1980–2018, the NH and SH cells contribute 40% and 60% of the total BDC change, respectively. The dynamical cooling in tropical T_{LS} in the past four decades is significant at the 90% confidence interval, as in 1980–2009 (Fu *et al* 2015). However, the NH contribution has now become significant at the 90% confidence interval for 1980–2018 while only the SH contribution was significant at the 90% level for 1980–2009 (Fu *et al* 2015). It should be noted that the trends for the combined period of 1980–2018 cannot be derived from those for the separate periods (e.g. figure 4) because of the evident nonlinear temporal variations and changes in behavior.

Using the relationship between tropical residual vertical velocity (w^*) at 70 hPa and T_{LS} from Fu *et al* (2015), a dynamical cooling of −0.08 K/decade in tropical T_{LS} trend corresponds to a mean change in w^* of 0.0046 mm/s/decade. Noting that the annual mean w^* at 70 hPa over the tropics is 0.288 mm s^{-1} from the ERA-Interim reanalysis, the relative strengthening of the BDC in terms of tropical residual vertical velocity at 70 hPa is 1.7% in the last 40 years, which is smaller than 2.1% for 1980–2009 (Fu *et al* 2015). This is consistent with a reduced role of ozone due to including its longer recovery era.

Figure 5 shows the monthly observed T_{LS} trends (left) and their dynamical (middle) and radiative (right) contributions for 1980–1999 (upper), 2000–2018 (middle), and 1980–2018 (lower) over SH high latitudes (dotted lines), NH high latitudes (dashed lines), and combined high latitudes (solid lines). The radiative contribution is obtained as the residual of the total minus the dynamical contribution. Note that the *y*-axis scale in figure 5 for 1980–2018 is finer than those for other two periods to more clearly show the results.

For the NH cell during 1980–1999, the BDC weakened in the Spring but strengthened in the Winter (Fu *et al* 2010, Free 2011, Fu *et al* 2015). For 2000–2018, the opposite occurred. For the entire period (i.e. 1980–2018), the NH cell displayed small changes in the Spring but accelerated in the Winter. The weakening (strengthening) of the BDC NH cell in the Spring for 1980–1999 (2000–2018) thus seems to be associated with the natural variability. This is supported by the fact that the NH radiative components do not change sign in March. Thus, the longer record

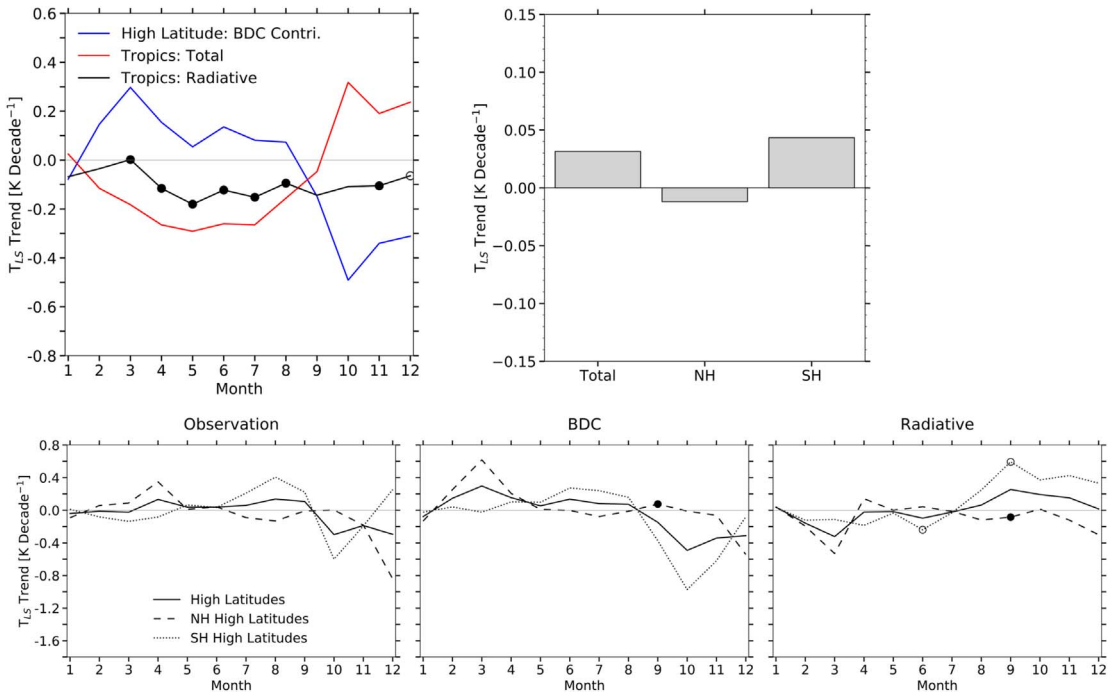

Figure 6. The upper left, upper right, and lower panels are the same as those in figures 3–5 for 2000–2018, respectively, but excluding the year 2002.

now available suggests that the weakening of the BDC NH cell in the Spring noted by Fu *et al* (2010), Free (2011), and Fu *et al* (2015), may be only a manifestation of natural variability. The NH cell of the BDC in the Winter is strengthening, weakening, and strengthening, respectively, for 1980–1999 (large in January), 2000–2018 (large in December), and 1980–2018 (large in January) (see figure 5). The change for 1980–2018 is suggestive of links to the increase of GHGs, assuming that 40 years are long enough to largely average out the impact of the natural variability such as the decadal variation of the North Atlantic Oscillations (e.g. Hu and Tung 2002, Omrani *et al* 2016, Hardiman *et al* 2017).

The SH cell of the BDC is strengthening, weakening, and strengthening, respectively, for 1980–1999 (large in August), 2000–2018 (large in October), and 1980–2018 (large in September—November). Figure 5 suggests that the large cooling during October—December in SH high latitudes shown in figure 1 for 2000–2018 is driven by changes of the BDC. It also indicates that the annual mean SH high-latitude cooling for 1980–1999 and 2000–2018 (figure 2) is caused by the ozone depletion and BDC weakening, respectively. The maximum SH radiative warming in September for 2000–2018 supports Solomon *et al* (2016) that healing of the Antarctic ozone layer has now begun to occur during the month of September.

An unusual sudden stratospheric warming occurred in Antarctica in 2002, which would lead to a spurious dynamical cooling trend in the SH high latitudes for 2000–2018. We repeat the analyses by removing the year 2002 (figure 6). Without 2002, while the results change little for 1980–2018 (not shown), the annual mean dynamical cooling (warming) in the SH high latitudes (tropics) becomes only one fourth of that for 2000–2018 including 2002 (figures 4 and 6). Noting the opposite signs of radiative components in the SH during August—December for the first versus second periods and their magnitudes with a factor of ~4 difference (figures 5 and 6), the changes of the BDC SH cell appear to be at least partly linked to ozone depletion and healing (see the modeling studies of Polvani *et al* 2018, Polvani *et al* 2019). It is also worth noting that by removing 2002, the SH radiative warming in September for 2000–2018 becomes significant at the 90% confidence level (figure 6). Both figures 5 and 6 show that the BDC changes mainly occur in the Winter and Spring seasons for both SH and NH cells during all three periods considered.

With the MSU/AMSU data in the last four decades (Santer *et al* 2019), the response of the BDC NH cell to the GHG increases since 1980 may be emerging. Although large dynamical trends are found in boreal spring over shorter periods, trends over the whole period remain very small for this season (figure 5). The SH cell is still the main contributor to the total BDC change in magnitude, but becomes statistically insignificant (figure 4), unlike that in the period of 1980–2009 (Fu *et al* 2015). This could partly be because BDC weakening in response to ozone healing cancels more of the strengthening during the ozone depletion period when the full record is considered.

4. Summary and conclusions

This study examines the BDC changes in the past four decades (1980–2018) as well as in the ozone depletion (1980–1999) and ozone healing (2000–2018) periods based on satellite MSU/AMSU T_{LS} observations and ERA-Interim reanalysis data. We show that the annual mean BDC has accelerated over 1980–2018 (at the 90% confidence level), as in 1980–2009 (Fu *et al* 2015). However, the NH contribution is significant at the 90% confidence interval for 1980–2018 while it was not for 1980–2009 (Fu *et al* 2015). This is because the weakening and strengthening of the BDC NH cell in the boreal Spring for the first and second periods, which are largely related to natural variability, cancel each other. At the same time, the SH contribution is significant at the 90% level for 1980–2009 (Fu *et al* 2015) but becomes insignificant for 1980–2018, a period of longer ozone healing. We derived a relative strengthening of ~1.7% per decade (40% from the NH cell and 60% from the SH cell) in the last four decades, which is smaller than 2.1% per decade for 1980–2009. The smaller relative strengthening in the former period could be related to the ozone healing since the beginning of the 21st century.

The annual mean BDC has accelerated for 1980–1999 but decelerated for 2000–2018. Almost all of the change comes from the SH cell for both periods, which is because the weakening (strengthening) of the NH cell in the boreal Spring largely cancels the strengthening (weakening) of the NH cell in the boreal Winter for 1980–1999 (2000–2018). The enhanced SH radiative warming in September for 2000–2018, which is significant at the 90% confidence level after excluding the year 2002, supports Solomon *et al* (2016) that healing of the Antarctic ozone layer has now begun to occur during the month of September.

With the MSU/AMSU data in the last four decades, the response of the BDC NH cell to GHG increases in the past four decades may be emerging. The observationally-derived changes of the BDC in the ozone depletion and healing periods also support the GCM and CCM predictions.

Acknowledgments

This research was supported by NASA grant 80NSSC18K1031, NSF grants AGS-1821437 and AGS-1848863, and NOAA Grant NA18OAR4310423. QF thanks the International Space Science Institute (ISSI) Tropical Width and its Impacts on the STratosphere (TWIST) project that partly stimulated this project.

Data availability statements

The data that support the findings of this study are available from the corresponding author upon reasonable request.

References

Appenzeller C, Holton J R and Rosenlof K H 1996 Seasonal variation of mass transport across the tropopause *J. Geophys. Res.* **101** 15071–8

Birner T 2010 Residual circulation and tropopause structure *J. Atmos. Sci.* **67** 2582–600

Bohlinger P, Sinnhuber B-M, Ruhnke R and Kirner O 2014 Radiative and dynamical contributions to past and future Arctic stratospheric temperature trends *Atmos. Chem. Phys.* **14** 1679–88

Brewer A W 1949 Evidence for a world circulation provided by measurements of helium and water vapour distribution in the stratosphere *Q. J. R. Meteorol. Soc.* **75** 351–63

Bunzel F and Schmidt H 2013 The Brewer-Dobson circulation in a changing climate: impact of the model configuration *J. Atmos. Sci.* **70** 1437–55

Butchart N *et al* 2006 Simulations of anthropogenic change in the strength of the Brewer-Dobson circulation *Clim. Dyn.* **27** 727–41

Butchart N 2014 The Brewer–Dobson circulation *Rev. Geophys.* **52** 157–84

Davis S M, Liang C K and Rosenlof K H 2013 Interannual variability of tropical tropopause layer clouds *Geophys. Res. Lett.* **40** 2862–6

Dee D P *et al* 2011 The ERA-Interim reanalysis: Configuration and performance of the data assimilation system *Q. J. R. Meteorol. Soc.* **137** 553–97

Dessler A E, Schoeberl M R, Wang T, Davis S M and Rosenlof K H 2013 Stratospheric water vapor feedback *Proc. Natl Acad. Sci.* **110** 18087–91

Dietmüller S, Garny H, Plöger F, Jöckel P and Cai D 2017 Effects of mixing on resolved and unresolved scales on stratospheric age of air *Atmos. Chem. Phys.* **17** 7703–19

Ding Q and Fu Q 2018 A warming tropical central Pacific dries the lower stratosphere *Clim. Dyn.* **50** 2813–27

Dobson G M B 1956 Origin and distribution of polyatomic molecules in the atmosphere *Proc. R. Soc.* **A236** 187–93

Engel A, Bönisch H, Ullrich M, Sitals R, Membrive O, Danis F and Crevoisier C 2017 Mean age of stratospheric air derived from AirCore observations *Atmos. Chem. Phys.* **17** 6825–38

Engel A *et al* 2009 Age of stratospheric air unchanged within uncertainties over the past 30 years *Nat. Geosci.* **2** 28–31

Eyring V *et al* 2005 A Strategy for process-oriented validation of coupled chemistry-climate models *Bull. Am. Meteorol. Soc.* **86** 1117–33

Free M 2011 The seasonal structure of temperature trends in the tropical lower stratosphere *J. Clim.* **24** 859–66

Fu Q 2013 Bottom up in the tropics *Nat. Clim. Change* **3** 957–8

Fu Q, Johanson C M, Wallace J M and Reichler T 2006 Enhanced mid-latitude tropospheric warming in satellite measurements *Science* **312** 1179–1179

Fu Q and Lin P 2011 Poleward shift of subtropical jets inferred from satellite-observed lower-stratospheric temperatures *J. Climate* **24** 5597–603

Fu Q, Lin P, Solomon S and Hartmann D L 2015 Observational evidence of strengthening of the Brewer-Dobson circulation since 1980 *J. Geophys. Res. Atmos.* **120** 10214–28

Fu Q, Solomon S and Lin P 2010 On the seasonal dependence of tropical lower-stratospheric temperature trends *Atmos. Chem. Phys.* **10** 2643–53

Fueglistaler S 2012 Stepwise changes in stratospheric water vapor? *J. Geophys. Res.* **117** 1–11

Garcia R R and Randel W J 2008 Acceleration of the Brewer-Dobson circulatio due to increase in greenhouse gases *J. Atmos. Sci.* **65** 2731–9

Garny H, Birner T, Bönisch H and Bunze F 2014 The effects of mixing on age of air *J. Geophys. Res.-Atmos.* **119** 7015–34

Gerber E P *et al* 2012 Assessing and understanding the impact of stratospheric dynamics and variability on the earth system *Bull. Am. Meteorol. Soc.* **93** 845–59

Haenel F J *et al* 2015 Reassessment of MIPAS age of air trends and variability *Atmos. Chem. Phys.* **15** 13161–76

Hall T M and Plumb R A 1994 Age as a diagnostic of stratospheric transport *J. Geophys. Res.* **99** 1059–70
Hardiman S, Lin P, Scaife A, Dunstone N and Ren H-L 2017 The influence of dynamical variability on the observed Brewer–Dobson circulation trend *Geophys. Res. Lett.* **44** 2885–92
Holton J R 1990 On the global exchange of mass between the stratosphere and troposphere *J. Atmos. Sci.* **47** 392–5
Holton J R, Haynes P H, McIntyre M E, Douglass A R, Rood R B and Pfister L 1995 Stratosphere-troposphere exchange *Rev. Geophys.* **33** 403–39
Hu Y and Fu Q 2009 Stratospheric warming in Southern Hemisphere high latitudes since 1979 *Atmos. Chem. Phys.* **9** 4329–40
Hu Y and Tung K K 2002 Interannual and decadal variations of planetary wave activity, stratospheric cooling, and northern hemisphere annular mode *J. Climate* **15** 1659–73
Ivy D J, Solomon S and Rieder H E 2016 Radiative and dynamical influences on polar stratospheric temperature trends *J. Clim.* **29** 4927–38
Johanson C M and Fu Q 2007 Antarctic atmospheric temperature trend patterns from satellite observations *Geophys. Res. Lett.* **34** L12703
Li F, Austin J and Wilson R J 2008 The strength of the Brewer-Dobson circulation in a changing climate: coupled chemistry-climate model simulations *J. Clim.* **21** 40–57
Lin P and Fu Q 2013 Changes in various branches of the Brewer-Dobson circulation from an ensemble of chemistry climate models *J. Geophys. Res. Atmos.* **118** 73–84
Lin P, Fu Q, Solomon S and Wallace J M 2009 Temperature trend patterns in Southern Hemisphere high latitudes: novel indicators of stratospheric change *J. Clim.* **22** 6325–41
Maycock A C *et al* 2018 Revisiting the mystery of recent stratospheric temperature trends *Geophys. Res. Lett.* **45** 9919–33
McLandress C, Jonsson A I, Plummer D A, Reader M C, Scinocca J F and Shepherd T G 2010 Separating the dynamical effects of climate change and ozone depletion: I. Southern Hemisphere stratosphere *J. Clim.* **23** 5002–20
McLandress C and Shepherd T G 2009 Simulated anthropogenic changes in the Brewer-Dobson circulation, including its extension to high latitudes *J. Clim.* **22** 1516–40
Mears C and Wentz F J 2017 A satellite-derived lower-tropospheric atmospheric temperature dataset using an optimized adjustment for diurnal effects *J. Clim.* **30** 7695–718
Oberlander S, Langematz U and Meul S 2013 Unraveling impact factors for future changes in the Brewer-Dobson circulation *J. Geophys. Res. Atmos.* **118** 10296–312
Okamoto K, Sato K and Akiyoshi H 2011 A study on the formation and trend of the Brewer-Dobson circulation *J. Geophys. Res.* **116** D10117
Oman L, Waugh D W, Pawson S, Stolarski R S and Newman P A 2009 On the influence of anthropogenic forcings on changes in the stratospheric mean age *J. Geophys. Res.* **114** D03105
Omrani N E, Bader J, Keenlyside N S and Manzini E 2016 Troposphere–stratosphere response to large-scale North Atlantic Ocean variability in an atmosphere/ocean coupled model *Clim. Dyn.* **46** 1397–415
Osso A, Sola Y, Rosenlof K, Hassler B, Bech J and Lorente J 2015 How robust are trends in the Brewer–Dobson circulation derived from observed stratospheric temperatures? *J. Clim.* **28** 3024–40
Pawson S *et al* 2000 The GCM-reality intercomparison project for SPARC (GRIPS): scientific issues and initial results *Bull. Am. Meteorol. Soc.* **81** 781–96
Ploeger F, Riese M, Haenel F, Konopka P, Müller R and Stiller G 2015 Variability of stratospheric mean age of air and of the local effects of residual circulation and eddy mixing *J. Geophys. Res.-Atmos.* **120** 716–33
Plumb R A 2002 Stratospheric transport *J. Met. Soc. Japan* **80** 793–809
Polvani L M *et al* 2019 Large impacts, past and future, of ozone-depleting substances on Brewer-Dobson circulation trends: a multi-model assessment *J. Geophys. Res.* **124** 6669–80
Polvani L M, Abalos M, Garcia R, Kinnison D and Randel W J 2018 Significant weakening of Brewer-Dobson circulation trends over the 21st century as a consequence of the Montreal Protocol *Geophys. Res. Lett.* **45** 401–9
Polvani L M, Waugh D W, Correa G J P and Son S W 2011 Stratospheric ozone depletion: the main driver of twentieth-century atmospheric circulation changes in the Southern Hemisphere *J. Clim.* **24** 795–812
Randel W J, Wu F, V mel H, Nedoluha G and Forster P 2006 Decreases in stratospheric water vapor after 2001: links to changes in the tropical tropopause and the Brewer–Dobson circulation *J. Geophys. Res.* **111** 1–11
Ray E A *et al* 2014 Improving stratospheric transport trend analysis based on SF6 and CO_2 measurements *J. Geophys. Res.: Atmos.* **119** 14110–28
Rind D, Suozzo R, Balachandran N K and Prather M J 1990 Climate change and the middle atmosphere: I. The doubled CO_2 climate *J. Atmos. Sci.* **47** 475–94
Santer B D *et al* 2019 Celebrating the anniversary of three key events in climate change science *Nat. Clim. Change* **9** 180–2
Shepherd T G 2008 Dynamics, stratospheric ozone, and climate change *Atmos.-Ocean* **46** 117–38
Shindell D T and Schmidt G A 2004 Southern Hemisphere climate response to ozone changes and greenhouse gas increases *Geophys. Res. Lett.* **31** L18209
Solomon S 1999 Stratospheric ozone depletion: a review of concepts and history *Rev. Geophys.* **37** 275–316
Solomon S, Ivy D, Gupta M, Bandoro J, Santer B, Fu Q, Lin P, Garcia R R, Kinnison D and Mills M 2017 Mirrored changes in Antarctic ozone and stratospheric temperature in the late 20th versus early 21st centuries *J. Geophys. Res. Atmos.* **122** 8940–50
Solomon S, Ivy D J, Kinnison D, Mills M J, Neely R R III and Schmidt A 2016 Emergence of healing in the Antarctic ozone layer *Science* **353** 269–74
Spencer R W, Christy J R and Braswell W D 2017 UAH version 6 global satellite temperature products: methodology and results. Asia-Pac *J. Atmos. Sci.* **53** 121–30
Stiller G P *et al* 2017 Shift of subtropical transport barriers explains observed hemispheric asymmetry of decadal trends of age of air *Atmos. Chem. Phys.* **17** 11177–92
Stiller G P *et al* 2012 Observed temporal evolution of global mean age of stratospheric air for the 2002 to 2010 period *Atmos. Chem. Phys.* **12** 3311–31
Thompson D W J and Solomon S 2005 Recent stratospheric climate trends as evidenced in radiosonde data: global structure and tropospheric linkages *J. Clim.* **18** 4785–95
Thompson D W J and Solomon S 2009 Understanding recent stratospheric climate change *J. Clim.* **22** 1934–43
Tseng H H and Fu Q 2017 Temperature control of the variability of tropical tropopause layer cirrus clouds *J. Geophys. Res. Atmos.* **122** 11062–75
Young P J, Rosenlof K H, Solomon S, Sherwood S C, Fu Q and Lamarque J-F 2012 Changes in stratospheric temperatures and their implications for changes in the Brewer–Dobson circulation, 1979–2005 *J. Clim.* **25** 759–1772
Yulaeva E, Holton J R and Wallace J M 1994 On the cause of the annual cycle in tropical lower-stratospheric temperatures *J. Atmos. Sci.* **51** 169–74
Zou C-Z, Goldberg M and Hao X 2018 New generation of US satellite microwave sounder achieves high radiometric stability performance for reliable climate change detection *Sci. Adv.* **4** eaau0049